Cross-Coupling in Coaxial Cavity Filters—A Tutorial Overview

J. Brian Thomas, *Member, IEEE*

***Abstract*—This paper presents a tutorial overview of the use of coupling between nonadjacent resonators to produce transmission zeros at real frequencies in microwave filters. Multipath coupling diagrams are constructed and the relative phase shifts of multiple paths are observed to produce the known responses of the cascaded triplet and quadruplet sections. The same technique is also used to explore less common nested cross-coupling structures and to predict their behavior. A discussion of the effects of nonzero electrical length coupling elements is presented. Finally, a brief categorization of the various synthesis and implementation techniques available for these types of filters is given.**

***Index Terms*—Coaxial cavity filter, cross-coupling, nested cross-coupling, tutorial.**

I. Introduction

"LIFE IS really simple, but we insist on making it complicated"—Confucius. This paper will attempt to provide a simplified, qualitative, and intuitive understanding of an important and complex topic in the field of microwave filters: cross-coupling, especially cross-coupling in coaxial cavity filters.

The ever increasing need for capacity in cellular and personal communications systems (PCSs) has led to more stringent requirements for basestation filters and duplexers. The transmit and receive bandpass filters composing basestation duplexers may have required rejection levels greater than 100 dB on one side of the passband and, at the same time, have very mild rejection requirements on the opposite side [1]. The technique of cross-coupling to produce asymmetric frequency responses has become popular for these applications because it concentrates the filter's ability to provide rejection only over the band where it is needed. This "concentration of rejection" means the filter's response is trimmed of unnecessary rejection anywhere it is not absolutely required, increasing the overall efficiency of the design. The tradeoff in slope between the bandpass filter's upper and lower skirt is optimized for the particular requirement. Fig. 1 shows a filter response with and without two transmission zeros on the upper skirt. Using the technique of cross-coupling to produce transmission zeros, the rejection above the passband is increased, while rejection below the passband it is relaxed. This can reduce the number of resonating elements required to meet a specification and this, in turn, reduces the insertion loss, size, and manufacturing cost of the design, though at the expense of topological complexity and, perhaps, development and tuning time.

Manuscript received January 31, 2002.

The author is with the Engineering Department, Baylor University, Waco, TX 76703 USA.

Digital Object Identifier 10.1109/TMTT.2003.809180

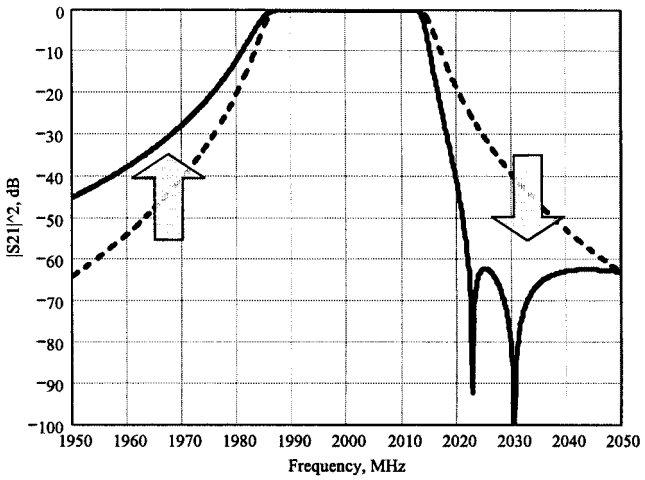

Fig. 1. Two possible filter responses, with (dashed line) and without (solid line) finite transmission zeros produced by cross-coupling. Note the increase in rejection above the passband and the relaxation in rejection below. This asymmetrical response concentrates a filter's ability to provide rejection only where it is required.

Not only has the industry seen electrical requirements become more stringent, but mechanical packaging requirements have become less flexible due to basestation miniaturization and multiple-sourcing considerations. The choices of overall size and shape and constraints in connector locations play a vital role in determining a filter's layout, topology, and internal structure. The differences can be substantial between a filter with connectors on the same surface versus opposite surfaces, all other parameters being equal. Cross-coupling provides an additional degree of flexibility in these design scenarios.

When all things are considered, the use of cross-coupling produces a superior design for many requirements. It is not surprising then that these circuits have been the subject of the field's best and brightest for some time [2]. However, despite the prodigious numbers of expert-level publications available, the nonspecialist RF engineer may be left with the impression that cross-coupling is unapproachably complex: likely a mixture of Maxwell's equations and Voodoo magic.

The intent of this paper is to provide a general understanding of some fundamental cross-coupling techniques by using multipath coupling diagrams to illustrate the relative phase shifts of multiple signal paths. This technique can also be used to understand, and aid in the design of, less common topologies using nested cross-couplings.

Section II reviews the simplified phase relationships of fundamental components in the equivalent circuit of coaxial cavity filters. Although the technique of cross-coupling can be

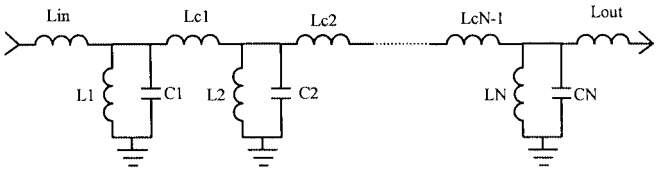

Fig. 2. Prototype equivalent circuit for combline or coaxial cavity filter. Shunt inductor/capacitor pairs represent individual resonating elements and the series inductors represent the dominantly magnetic coupling between resonators.

used with other types of filter realizations, (such as dielectric resonators, microstrip, or waveguide) special attention will be given to coaxial cavity filters because of their dominant role in wireless basestation filter applications.

Section III illustrates the multipath coupling diagram approach to describe the operation of well-known cascaded triplet (CT) and cascaded quadruplet (CQ) sections. The techniques of Section III require slight modification for realizations other than coaxial cavities; however, these are beyond the scope of this tutorial.

In Section IV, less common nested structures are explored, similar to the design of [3], where a five-section dielectric resonator filter with three transmission zeros is described. Section V gives a very broad description of the various implementation techniques in use today. Special focus will be given to methods accessible to most RF engineers. The conclusions are summarized in Section VI.

II. Phase Relationships

Combline and coaxial cavity filters may be represented by the prototype equivalent circuit of Fig. 2 [4]. Although simple lumped components are being used to represent three-dimensional structures with complex field patterns, nonetheless, they are useful and illustrative for purposes of this tutorial.

The shunt inductor/capacitor pairs represent individual resonating elements and the series inductors represent the dominantly magnetic coupling between resonators. The total coupling between adjacent resonators has both magnetic and electric components. However, these are out of phase with each other; the total coupling is the magnetic coupling less the electric coupling [5]. This is the reason a tuning screw placed between the *open* ends of two resonators increases the coupling between them (see Fig. 3). The screw decreases the electric coupling and, hence, increases the total coupling (less is subtracted from the total). By the same reasoning, a decoupling wall between the shorted ends of two resonators decreases the overall coupling by decreasing the magnetic coupling. For a more rigorous treatment of the coupling phenomenon, see [6]–[9].

The off-resonance (away from the passband) behavior of the components of Fig. 2 is utilized to produce the destructive interference resulting in transmission zeros and, therefore, needs to be understood. Let the phase component of the S-parameters S_{21} and S_{11} be denoted Φ_{21} and Φ_{11}, respectively. Consider the series inductor of Fig. 4 as a two-port device. A signal entering port 1 will undergo a phase shift upon exiting port 2. This is Φ_{21}, and it tends toward $-90°$. The fact that the magnitude of S_{21} is quite small at this point is not problematic in that the

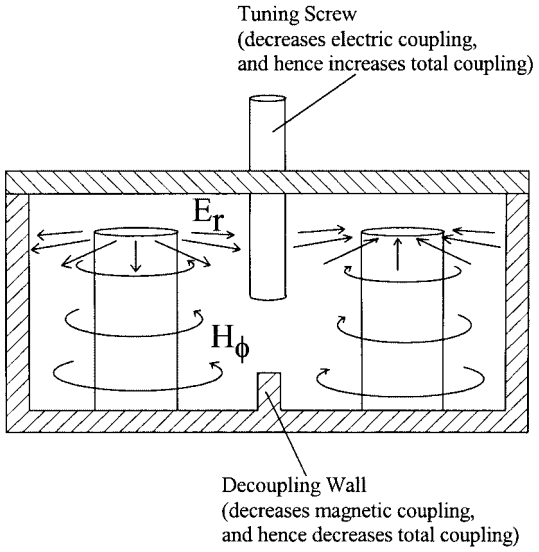

Fig. 3. Coupling fields between *adjacent* resonators. Total coupling may be affected by decoupling walls and/or tuning screws.

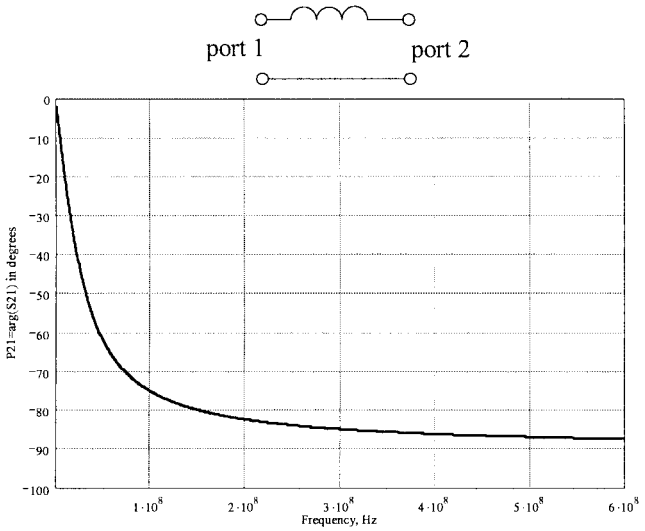

Fig. 4. Primary coupling between coaxial cavity resonators may be modeled as a series inductor. When considered as a two-port device, the phase of S_{21} (Φ_{21}) approaches $-90°$.

off-resonance behavior is what is of concern. It should be emphasized that, although this phase shift only *approaches* $-90°$ and, in general, may be much less, for purposes of general understanding, the approximation of $-90°$ is quite useful. Thus,

$$\Phi_{21} \approx -90° \text{ (for series inductors).} \tag{1a}$$

The shunt inductor/capacitor pairs of Fig. 2 (resonators) can also be thought of as two-port devices. However, the phase shift at off-resonance frequencies is dependent on whether the signal is above or below resonance (see Fig. 5). For signals below the resonant frequency (below the passband), the phase shift tends toward $+90°$. However, for signals above resonance, the phase shift tends toward $-90°$. This behavior is due to the simple fact that below resonance, the resonator is dominantly inductive and an inductor in shunt is the dual of a capacitor in series. Similarly for frequencies above resonance; the resonator is dominantly

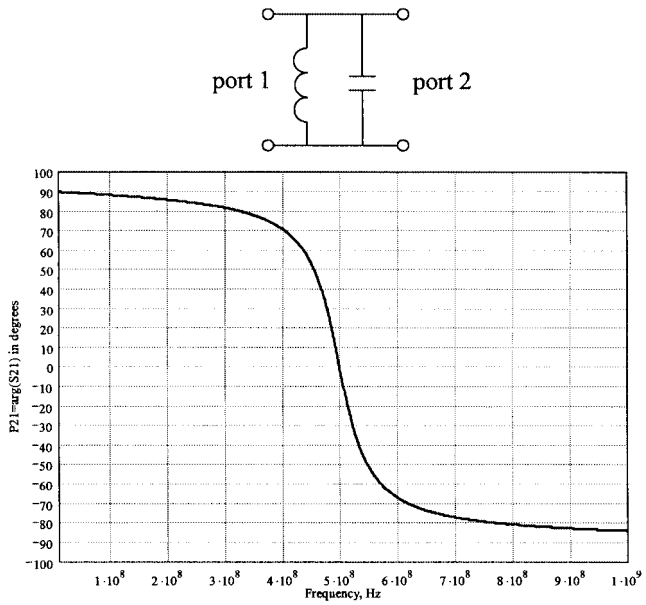

Fig. 5. Coaxial cavity resonators may be modeled as shunt inductor/capacitor pairs. When considered a two-port device, phase Φ_{21} approaches $\pm 90^\circ$ away from resonance, and passes through 0° at the resonant frequency.

capacitive and a shunt capacitor is the dual of a series inductor. Thus,

$$\Phi_{21} \approx +90^\circ \text{ (for resonators below resonance)} \quad (1b)$$

$$\Phi_{21} \approx -90^\circ \text{ (for resonators above resonance).} \quad (1c)$$

Although there are no series capacitors in Fig. 2, the series capacitor is an important cross-coupling device. The phase shift is

$$\Phi_{21} \approx +90^\circ \text{ (for series capacitors).} \quad (1d)$$

These phase shifts should not be confused with coupling coefficients commonly found in the literature, which may be of opposite sign as the phase shift of (1a)–(1d).

III. Multipath Coupling Diagrams

A. CT With Inductive Cross-Coupling

Consider the three resonator structure of Fig. 6(a) and (b), which represents a CT section using an inductive cross-coupling between resonators 1 and 3. The resonators of the equivalent circuit (Fig. 2) have been replaced by circles, but the inter-resonator inductors remain shown. Using the relationships of Section II, the phase shifts can be found for the two possible signal paths. Path 1–2–3 is the primary path, and path 1–3 is the secondary path that follows the cross-coupling. When summing the phase-shift contributions of the individual components, the contributions from resonators 1 and 3 are not required. Both paths share a common beginning and ending location; only the contribution of circuit elements *internal* to resonators 1 and 3 need to be considered. (Indeed, 1 and 3 need not even *be resonators*; the signals can be combined at the input or output of the filter itself (see [3]).) Furthermore, resonator 2 must be considered both above and below resonance. Table I shows these results.

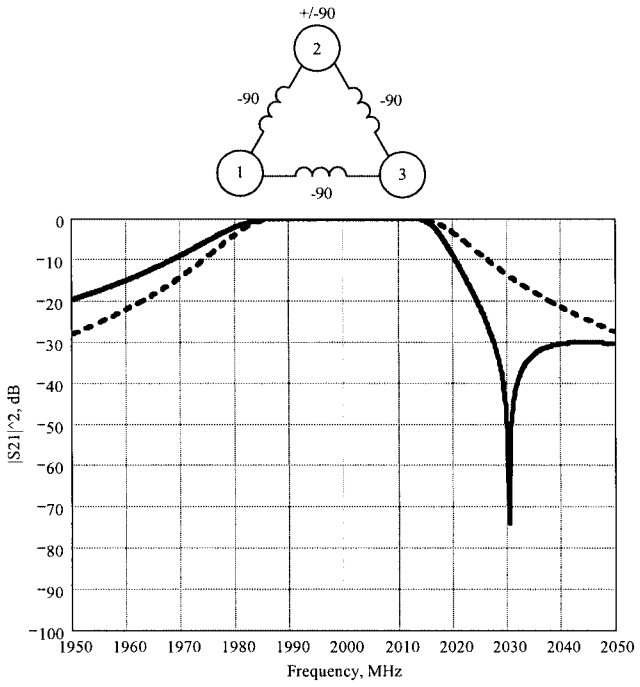

(a)

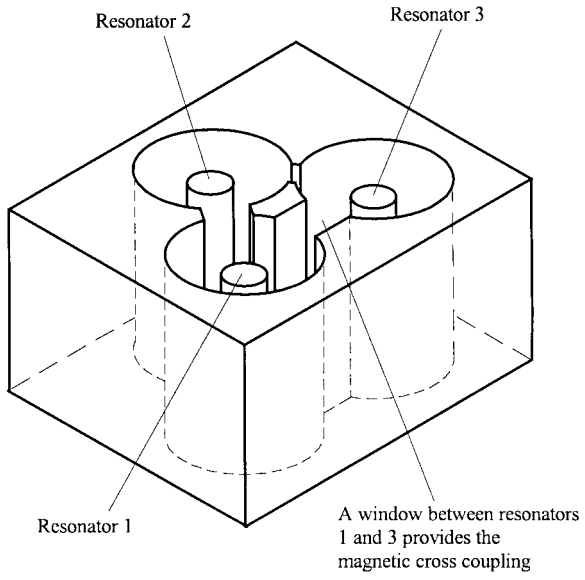

(b)

Fig. 6. (a) Multipath coupling diagram for CT section with *inductive* cross-coupling and possible frequency response including transmission zero (solid line). (b) Physical representation of CT section of (a).

Below resonance, the two paths are in phase, but above resonance, the two paths are 180° apart. This is exactly the case at one frequency only (here, approximately 2030 MHz), but is approximately the case for frequencies in the region (approximately 2020–2040 MHz). This destructive interference causes a transmission zero or null on the upper skirt. Stronger coupling between 1 and 3 causes the zero to move up the skirt toward the passband. Decreasing the coupling moves it farther down the skirt. This type of cross-coupling can be realized by a window between the cavities in the same way the primary coupling between resonator 1 and 2 or between 2 and 3 is realized. This is

TABLE I
TOTAL PHASE SHIFTS FOR TWO PATHS IN A CT SECTION WITH INDUCTIVE CROSS-COUPLING [SEE FIG. 6(a)]

	Below Resonance	Above Resonance
Path 1-2-3	-90°+90°-90° = -90°	-90°-90°-90° = -270°
Path 1-3	-90°	-90°
Result	In phase	Out of phase

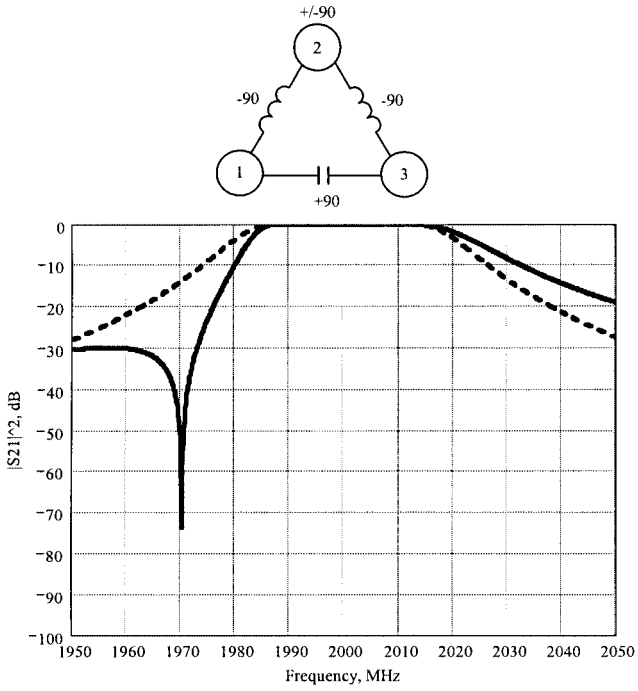

Fig. 7. Multipath coupling diagram for CT section with *capacitive* cross-coupling and possible frequency response including transmission zero (solid line). Also shown is the standard Chebyshev response without cross-coupling (dashed line).

advantageous in that no additional components are required [see Fig. 6(b)].

B. CT With Capacitive Cross-Coupling

In Fig. 7, the inductive cross-coupling between resonator 1 and 3 has been replaced with a capacitive probe. The phase shifts for the two possible signal paths are given in Table II. Again, path 1–2–3 is the primary path and is no different than in Table I. Path 1–3 is the secondary path and now has a +90° (positive) phase shift. Thus, for a capacitive cross-coupling, the destructive interference occurs *below* the passband.

C. CQ With Inductive Cross-Coupling

In Fig. 8, the four-resonator scenario known as the CQ is shown with an inductive cross-coupling. The primary path in this case is 1–2–3–4; the secondary path 1–4, therefore, bypasses two resonators. As Table III shows, transmission zeros are not produced at *any real* frequencies above or below the passband. However, zeros at imaginary frequencies can be produced, which have the effect of flattening the group delay over the passband. These types of responses are useful in extremely linear systems using feed-forward amplifiers. The flattening of

TABLE II
TOTAL PHASE SHIFTS FOR TWO PATHS IN A CT SECTION WITH CAPACITIVE CROSS-COUPLING (SEE FIG. 7)

	Below Resonance	Above Resonance
Path 1-2-3	-90°+90°-90° = -90°	-90°-90°-90° = -270°
Path 1-3	+90°	+90°
Result	Out of phase	In phase

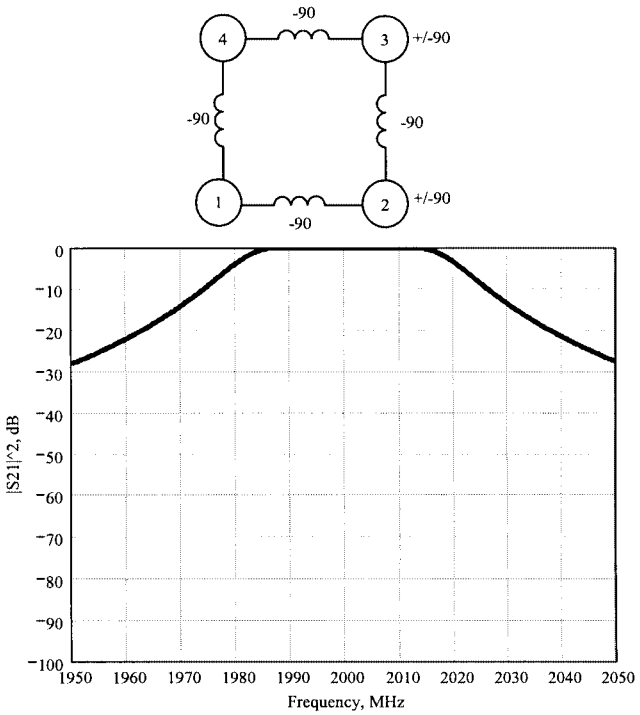

Fig. 8. Multipath coupling diagram for CQ section with inductive cross-coupling and possible frequency response.

TABLE III
TOTAL PHASE SHIFTS FOR TWO PATHS IN A CQ SECTION WITH INDUCTIVE CROSS-COUPLING (SEE FIG. 8)

	Below Resonance	Above Resonance
Path 1-2-3-4	-90°+90°-90°+90° = -90° = -90°	-90°-90°-90°-90°-90° = -450°=-90°
Path 1-4	-90°	-90°
Result	In phase	In phase

the group delay also has the effect of flattening the insertion loss. Midband losses increase slightly while band-edge rolloff effects are decreased.[1] These effects are not apparent from this analysis. See [10] and [11] for a more detailed analysis of filters with transmission zeros at imaginary frequencies.

D. CQ With Capacitive Cross-Coupling

Replacing the inductive element between resonators 1 and 4 with a capacitive probe, the other type of CQ is formed. This topology is particularly interesting, as Table IV shows, because transmission zeros are produced *both* above and below the passband (see Fig. 9).

[1]R. Wenzel, "Designing microwave filters, couplers and matching networks," a video tutorial published by Besser Associates, Los Altos, CA, 1986.

TABLE IV
TOTAL PHASE SHIFTS FOR TWO PATHS IN A CQ SECTION WITH CAPACITIVE CROSS-COUPLING (SEE FIG. 9)

	Below Resonance	Above Resonance
Path 1-2-3-4	-90°+90°-90°+90° = -90° = -90°	-90°-90°-90°-90°-90° = -450°=-90°
Path 1-4	+90°	+90°
Result	Out of phase	Out of phase

IV. NESTED STRUCTURES

It has been shown that two signal paths can be combined to produce a transmission zero. In this section, nested structures having three or more signal paths will be explored. Consider first the circuit of Fig. 10. The outer path 1–2–3 combines with 1–3 to form one transmission zero. Simultaneously, the interior path 1–3–4 combines with the innermost path 1–4 to produce a second transmission zero. Both are on the upper skirt. See Table V.

In the same way, the circuit of Fig. 11 produces two transmission zeros on the lower skirt. Key to its function is the capacitive cross-coupling between resonators 1 and 3 (see Table VI). These two circuits are especially useful in duplexer designs due to their similar topology and symmetry in response.

The multipath coupling diagram approach can also be used to understand the operation of some very interesting structures described in [3], although in it, the filters are realized with dielectric resonators instead of coaxial resonators.

Two possible coaxial realizations of a five-section three-transmission-zero filter are shown in Fig. 12(a) and (b). These are the only two configurations for achieving all three zeros on the same side of the passband. Other combinations exist that produce two zeros above and one below, for example. Tables VII and VIII show the phase relationships of Fig. 12 (a) and (b), respectively. Of particular interest is the circuit of 12(b) because it may be realized using all window couplings.

For some filter topologies having more than two possible signal paths [as in Fig. 12(a)], the question may be raised as to why the outermost and innermost paths do not also combine to produce an additional transmission zero. To produce a cancellation, the two paths must not only be opposite in phase, but equal in magnitude. A signal at an off-resonance frequency will be partially attenuated by every resonator in its path, therefore, the outermost and innermost paths will be of vastly different magnitude, regardless of phase.

As a working verification of this nested cross-coupling method, see Fig. 13. This eight-resonator filter was developed using the topologies of Figs. 10 and 11 combined. Resonators 1–4 produce both transmission zeros below the band, and resonators 5–8 produce both zeros above the band (special thanks to J. Roberds, Commercial Microwave Technology Inc., Rancho Cordova, CA, for this measured data).

V. FILTER IMPLEMENTATION

There is a multitude of important topics in the field of filter design and implementation such as the determination of the number of cavities and transmission zeros required to meet a specification, stopband requirements, and resonator design for proper frequency and Q_u operation, high power-handling considerations, and others. The reader is referred to [5], [12], and [13] as sources for designing microwave filters. These sources present much general material over a range of technical levels.

Limiting the scope of this tutorial to understanding the relationship between a cross-coupled filter circuit's topology and

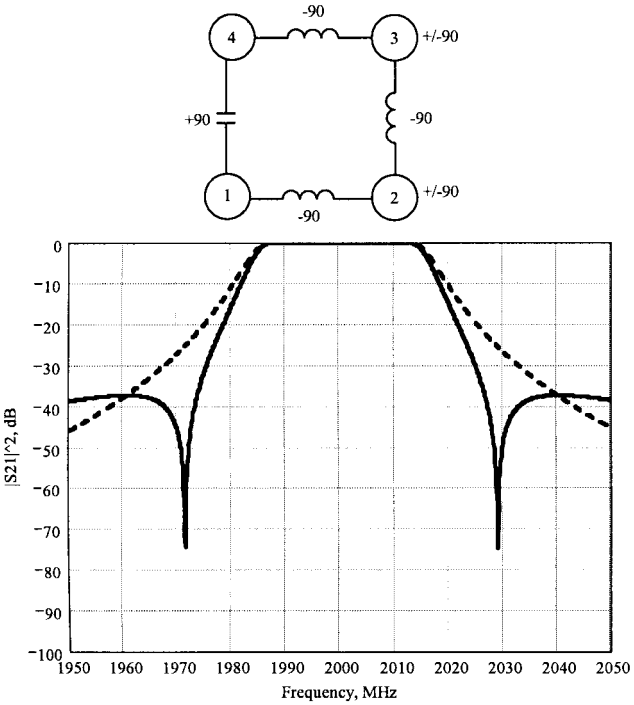

(a)

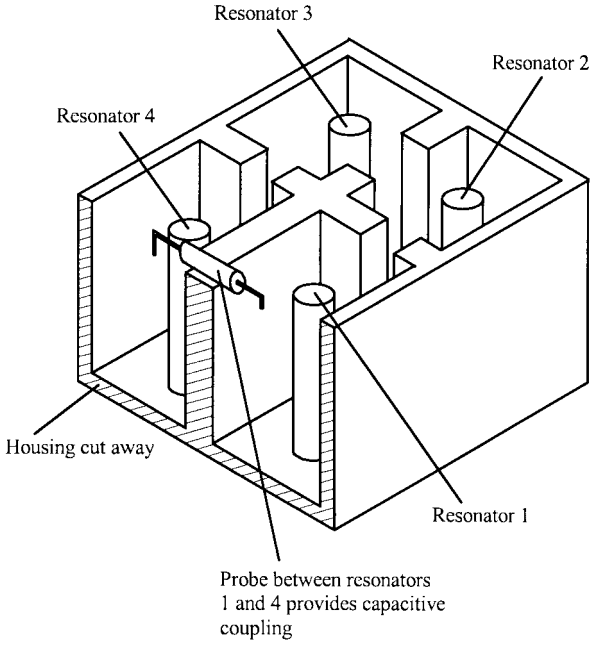

(b)

Fig. 9. (a) Multipath coupling diagram for CQ section with capacitive cross-coupling and possible frequency response. Transmission zeros are produced both above and below the passband (solid line). Compare to standard Chebyshev response (dashed line). (b) Physical representation of CQ section of (a). Here, the capacitive probe is formed from a length of semirigid coaxial cable with the outer conductor and insulator removed from the ends.

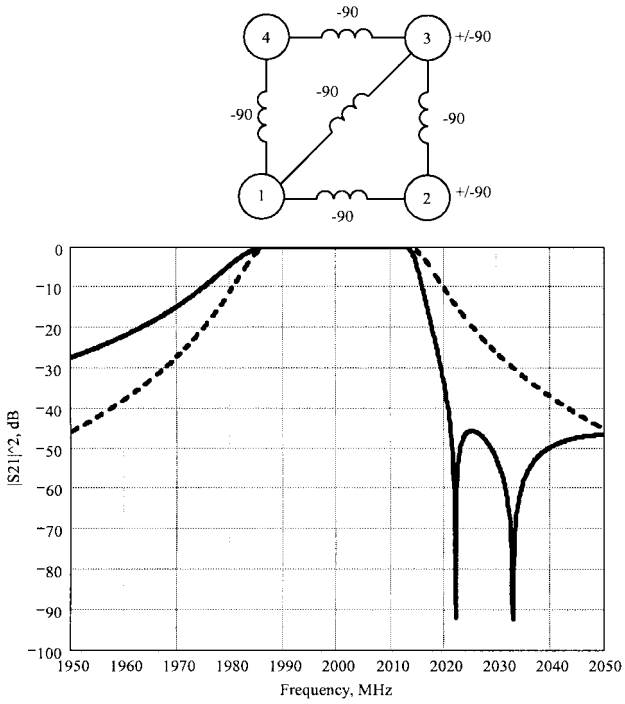

Fig. 10. Nested cross-coupling to produce two high-skirt transmission zeros (solid line). Compare to standard Chebyshev response (dashed line).

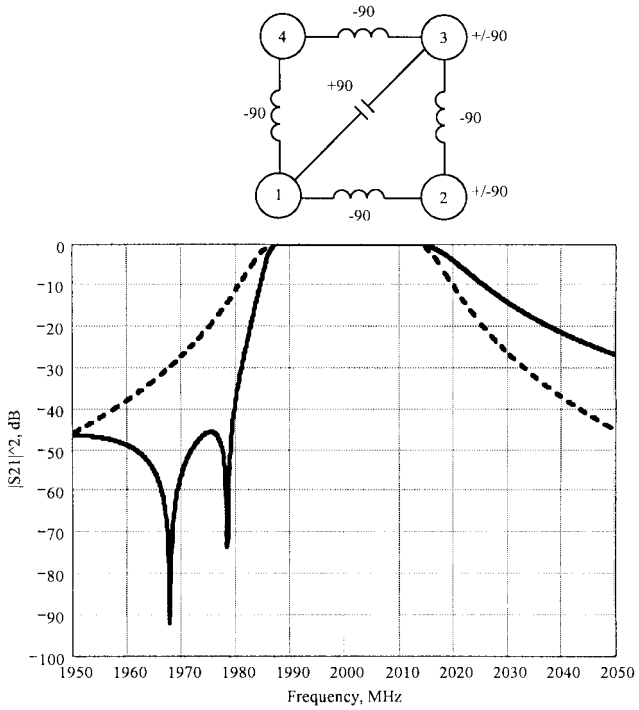

Fig. 11. Nested cross-coupling to produce two low-skirt transmission zeros (solid line). Compare to standard Chebyshev response (dashed line).

TABLE V
TOTAL PHASE SHIFTS FOR THREE PATHS OF THE CIRCUIT IN FIG. 10

	Below Resonance	Above Resonance
Path 1-2-3	-90°+90°-90° = -90°	-90°-90°-90° = -270°
Path 1-3	-90°	-90°
Result	In phase	Out of phase
Path 1-3-4	-90°+90°-90° = -90°	-90°-90°-90° = -270°
Path 1-4	-90°	-90°
Result	In phase	Out of phase

TABLE VI
TOTAL PHASE SHIFTS FOR THREE PATHS OF THE CIRCUIT IN FIG. 11

	Below Resonance	Above Resonance
Path 1-2-3	-90°+90°-90° = -90°	-90°-90°-90° = -270°
Path 1-3	+90°	+90°
Result	Out of phase	In phase
Path 1-3-4	+90°+90°-90° = +90°	+90°-90°-90° = -90°
Path 1-4	-90°	-90°
Result	Out of phase	In phase

its frequency response, a natural quantitative question arises; to what degree and in what sense are the various resonators coupled to one another for a given response? The answer to this question contains all the information required to describe the bandwidth and presence of any transmission zeros (at either real or imaginary frequencies). These couplings can be described by coupling coefficients or coupling bandwidths, where the coupling bandwidth equals the coupling coefficient multiplied by the design bandwidth. For an N resonator filter, these bandwidths can be arranged in an $N \times N$ coupling-bandwidth matrix. Each coupling bandwidth is readily measurable with a vector network analyzer and is, therefore, immediately useful in the development and production tuning of microwave filters (see [14] for a unified approach to the technique of using coupling coefficients with coupled resonator filters).

The methods for obtaining the coupling-bandwidth matrix required for a given frequency response may be broadly categorized into the following three categories:

1) direct synthesis;
2) low-pass prototype transformations;
3) optimization methods.

A. Direct Synthesis

The direct analytical synthesis of coupling coefficients for a given response has been presented in Levy's work given in [15]. This work provided an analytical alternative to applying matrix rotations to the canonic form of the filter, as had been earlier proposed in [16]–[18]. Unfortunately, this direct method is only applicable to the CQ filters, as shown in Figs. 8 and 9. The author is not aware of any closed-form solutions that are capable of generating a coupling matrix for the nested structures of Section IV. Analytical methods exist for CT and CQ structures only. Due to the comprehensive coverage of this method in the literature, no further discussion will be offered here.

B. Low-Pass Prototype Transformations

The method of transforming a low-pass prototype circuit into a bandpass filter scaled in frequency and impedance is an old approach that fills many textbooks on filter design. However, the limitations on this approach are that the result is a lumped-element filter that eventually must be approximated by distributed components. Furthermore, although elliptic function filters may

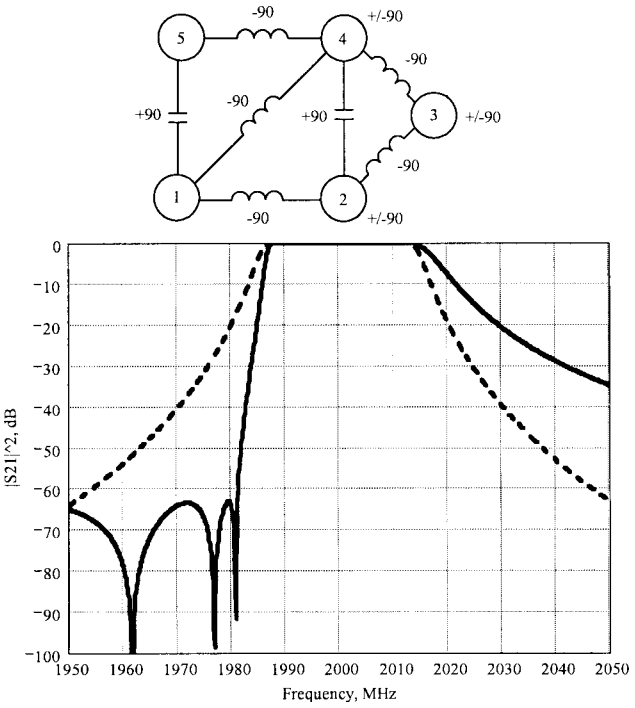

(a)

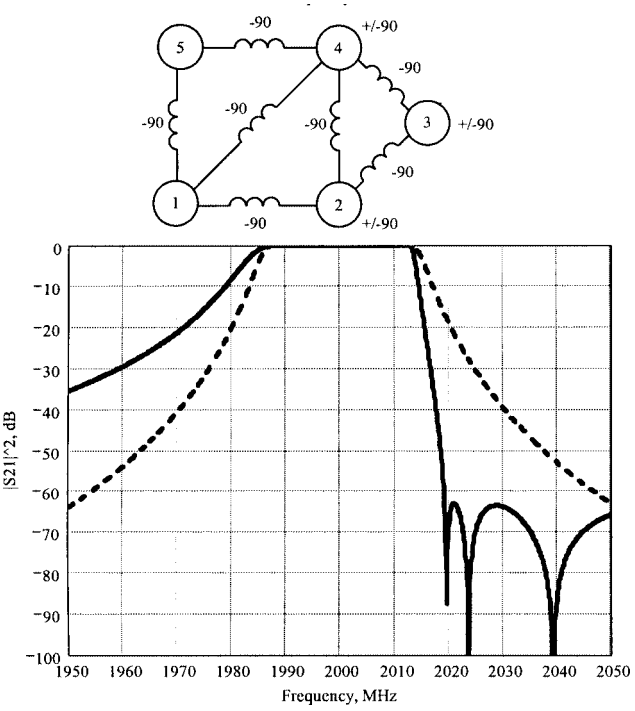

(b)

Fig. 12. (a) and (b) Two possible five-section three-transmission-zero realizations. All the couplings between resonators of circuit (b) may be realized with iris coupling, making this topology particularly attractive from a manufacturing point-of-view. In both cases, the standard five-cavity Chebyshev response is shown (dashed line) for reference.

be similar in that they utilize transmission zeros at finite frequencies, there are not straightforward design tables from which to select cross-coupled designs. If using this "recipe" approach, the choices are limited to standard ladder networks (Chebyshev, Butterworth, etc.) and elliptic function filters. Understanding of the methodology of using low-pass prototypes, however, is

TABLE VII
TOTAL PHASE SHIFTS FOR FOUR PATHS OF THE CIRCUIT IN FIG. 12(a)

	Below Resonance	Above Resonance
Path 2-3-4	-90°+90°-90° = -90°	-90°-90°-90° = -270°
Path 2-4	+90°	+90°
Result	Out of phase	In phase
Path 1-2-4	-90°+90°+90° = +90°	-90°-90°+90° = -90°
Path 1-4	-90°	-90°
Result	Out of phase	In phase
Path 1-4-5	-90°+90°-90° = -90°	-90°-90°-90° = -270°
Path 1-5	+90°	+90°
Result	Out of phase	In phase

TABLE VIII
TOTAL PHASE SHIFTS FOR FOUR PATHS OF THE CIRCUIT IN FIG. 12(b)

	Below Resonance	Above Resonance
Path 2-3-4	-90°+90°-90° = -90°	-90°-90°-90° = -270°
Path 2-4	-90°	-90°
Result	In phase	Out of phase
Path 1-2-4	-90°+90°-90° = -90°	-90°-90°-90° = -270°
Path 1-4	-90°	-90°
Result	In phase	Out of phase
Path 1-4-5	-90°+90°-90° = -90°	-90°-90°-90° = -270°
Path 1-5	-90°	-90°
Result	In phase	Out of phase

an important starting point for beginning filter designers due to the numerous allusions and references to the method found throughout the literature (see [5] and [13]).

C. Optimization Methods

Atia presented a "synthesis by optimization" method [19] in which the elements of the coupling matrix were simply given an initial gross approximation as either 1, 0, or -1. A pair of noncoupled resonators would have a coupling coefficient of zero (0), a pair with positive coupling (inductive) would be initially approximated as 1, and negative coupling (capacitive) would be initially approximated by -1. An optimization routine is then applied only at the poles and zeros, i.e., only at the frequencies where S_{11} (poles) and S_{21} (zeros) are numerically zero. Since the locations of the poles and zeros, together with the number of resonators N, uniquely determine the transfer function of the filter, these are the only frequencies for which optimization is required. The elements of the coupling matrix quickly converge to the correct values required to produce the specified transfer function (frequency response).

An analogous process using a linear microwave circuit simulator would be to add cross-coupling elements to a linear simulation of a standard Chebyshev filter. Using this method, the cross-coupling circuit elements can be lumped or a lumped/distributed combination. The elements should first be chosen such that they only minimally disturb the standard Chebyshev response. In the limit, this would approach a coupling coefficient of zero (a very small capacitor or very large inductor). These cross-coupling elements can then be adjusted manually or by

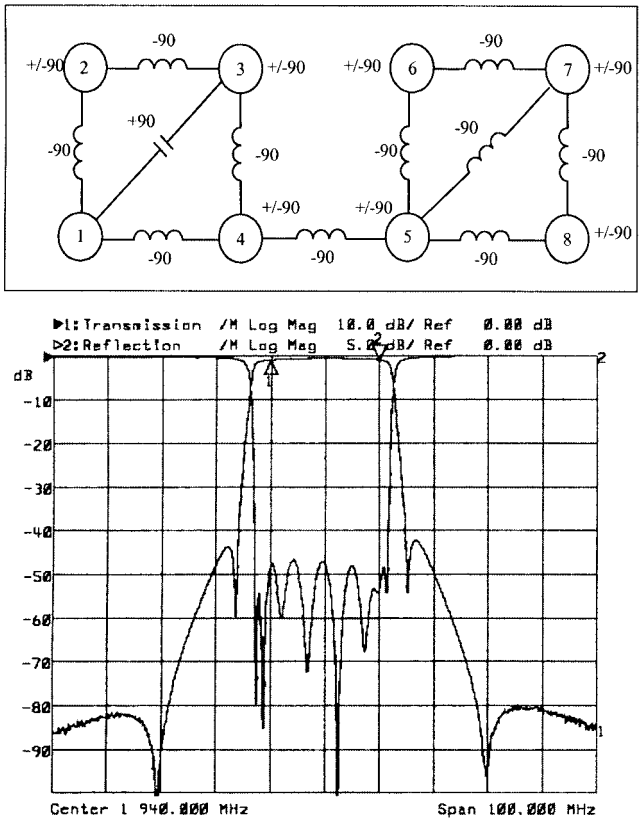

Fig. 13. Multipath coupling diagram and measured data for an eight-resonator filter. The design utilizes the nested cross-coupling techniques of Section IV.

using optimization routines. As the cross-coupling elements are adjusted, the tuned response of the filter will degrade. However, the tuning can be recovered quickly by retuning only the elements that are involved in the production of the transmission zero. As an example, consider an $N = 5$ filter with a cross-coupling from resonator 2 to 4. Adjusting the value of the 2–4 cross-coupling will detune the response, but it can be recovered by compensating resonators 2 and 4 and couplings 2–3 and 3–4 only.

The distributed nature of the cross-coupling elements themselves requires they have a nonzero electrical length. Taking these lengths into account will result in coupling-bandwidth information directly usable in the development and tuning process. In the analysis of Section III, phase shift was achieved purely from the reactance of the inductor or capacitor, not from its electrical length. However, the total phase contribution will consist of the reactive element *plus* any associated distributed contributions.

A common technique for realizing a capacitive cross-coupling is to strip the outer conductor away from the ends of a section of semirigid coaxial cable, such as RG141. This provides a probe, isolated from the housing, that is easily formed and adjusted (see Fig. 14).

The electrical length of this probe should be included in the simulation, and the capacitance on each end estimated. This electrical length should be kept short if the intent is to realize the response of Fig. 7 (a lower skirt transmission zero); however, by increasing the length by odd multiples of 180°, the response of Fig. 6 can be achieved (i.e., the response of an

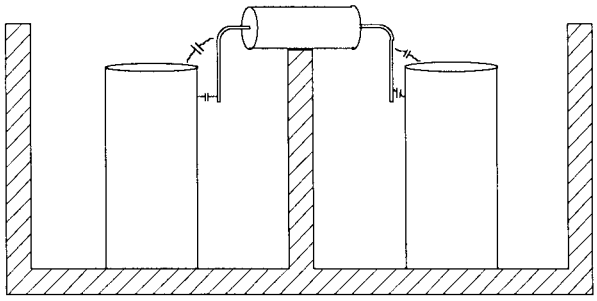

Fig. 14. Capacitive cross-coupling probe formed from semirigid coaxial cable between two *nonadjacent* resonators.

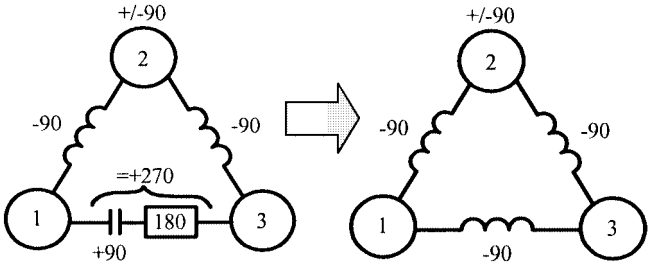

Fig. 15. (a) and (b) Importance of including the electrical length of the cross-coupling component is illustrated by showing that a capacitive probe, if electrically long, can have the same phase relationship as a lumped inductor.

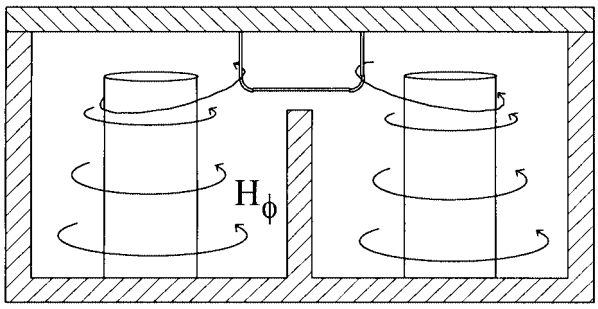

Fig. 16. Inductive cross-coupling loop between the *nonadjacent* resonators.

inductive cross-coupling, an *upper* skirt transmission zero). In this case, the multipath coupling diagram might look like the one shown in Fig. 15(a), but have the response of Fig. 15(b).

For inductive cross-couplings, the ideal coupling structure is a window and iris combination because it has fewer mechanical parts than its alternative, i.e., a coupling loop. If the layout does not allow for iris coupling, a simple loop placed normal to the magnetic field will provide the desired effect (see Fig. 16).

Finally, the tuned circuit is ready to have its coupling-bandwidth matrix extracted. This is accomplished by temporarily placing a short circuits in parallel with the resonators and successively removing them while making reflected S_{11} phase measurements. For the coupling between the first and second resonator, this measurement is of the bandwidth required for the reflected signal to undergo a 180° phase shift. Couplings that are more interior can vary from this. This measurement is performed both in the computer simulation environment (for the determination of the matrix) and on the bench (for the development of the prototype) (see [14] and [20] for more on this technique).

VI. Conclusion

A review of the importance, need, and benefits of using cross-coupling in coaxial cavity filter design has been presented. An approximate model for understanding the phase-shift contributions of relevant lumped-element components has been used with a multipath coupling diagram approach to explain the behavior of well-known triplet and quadruplet sections, as well as to predict the response of less common nested structures. This technique is extremely useful for determining an optimal cavity layout for given electrical and mechanical specifications. Finally, several design approaches have been categorized, including some numerical methods suitable for the nonspecialist RF engineer.

Acknowledgment

The author would like to thank J. Roberds, Commercial Microwave Technology Inc., Rancho Cordova, CA, and C. Hole, Remec Airtech, Aylesbury, U.K., for many fruitful discussions on this topic.

References

[1] R. J. Cameron, "General coupling matrix synthesis methods for Chebyshev filtering functions," *IEEE Trans. Microwave Theory Tech.*, vol. 47, pp. 433–442, Apr. 1999.

[2] R. Levy and S. B. Cohn, "A history of microwave filter research, design, and development," *IEEE Trans. Microwave Theory Tech.*, vol. MTT-32, pp. 1055–1067, Sept. 1984.

[3] J.-F. Liang and W. D. Blair, "High-Q $\mathrm{TE}01$ mode DR filters for PCS wireless base stations," *IEEE Trans. Microwave Theory Tech.*, vol. 46, pp. 2493–2500, Dec. 1998.

[4] R. Wenzel, "Synthesis of combline and capacitively loaded interdigital bandpass filters of arbitrary bandwidth," *IEEE Trans. Microwave Theory Tech.*, vol. MTT-19, pp. 678–686, Aug. 1971.

[5] R. W. Rhea, *HF Filter Design and Computer Simulation*. Atlanta, GA: Noble, 1994, p. 321.

[6] X.-P. Liang and K. A. Zaki, "Modeling of cylindrical dielectric resonators in rectangular waveguides and cavities," *IEEE Trans. Microwave Theory Tech.*, vol. 41, p. 2174, Dec. 1993.

[7] H. W. Yao, C. W. Wang, and K. A. Zaki, "Effects of tuning structures on combline filters," *IEEE Trans. Microwave Theory Tech.*, vol. 43, pp. 2824–2830, Dec. 1995.

[8] J. M. Chuma and D. Mirshekar-Syahkal. (2002) Effects of walls on coupling between coupled combline resonators. *Proc. Inst. Elect. Eng.* [Online] No. 20 020 180.

[9] H.-W. Yao, K. A. Zaki, A. E. Atia, and R. Hershtig, "Full wave modeling of conducting posts in rectangular waveguides and its applications to slot coupled combline filters," *IEEE Trans. Microwave Theory Tech.*, vol. 43, pp. 2824–2830, Dec. 1995.

[10] R. Levy, "Filters with single transmission zeros at real or imaginary frequencies," *IEEE Trans. Microwave Theory Tech.*, vol. MTT-24, pp. 172–181, Apr. 1976.

[11] G. Macchiarella, "An original approach to the design of bandpass cavity filters with multiple couplings," *IEEE Trans. Microwave Theory Tech.*, vol. 45, pp. 179–187, Feb. 1997.

[12] I. Hunter, *Theory and Design of Microwave Filters*. London, U.K.: IEE Press, 2001.

[13] G. L. Matthaei, L. Young, and E. M. T. Jones, *Microwave Filters, Impedance-Matching Networks and Coupling Structures*. New York: McGraw-Hill, 1964.

[14] J. B. Ness, "A unified approach to the design, measurement, and tuning of coupled-resonator filter," *IEEE Trans. Microwave Theory Tech.*, vol. 46, pp. 343–351, Apr. 1998.

[15] R. Levy, "Direct synthesis of cascaded quadruplet (CQ) filters," *IEEE Trans. Microwave Theory Tech.*, vol. 43, pp. 2940–2945, Dec. 1995.

[16] A. E. Atia and A. E. Williams, "Narrow-bandpass waveguide filters," *IEEE Trans. Microwave Theory Tech.*, vol. MTT-20, pp. 258–265, Apr. 1972.

[17] R. J. Cameron and J. D. Rhodes, "Asymmetric realizations for dual-mode bandpass filters," *IEEE Trans. Microwave Theory Tech.*, vol. MTT-29, pp. 51–58, Jan. 1981.

[18] R. Levy, "Synthesis of general asymmetric singly and doubly terminated cross-coupled filters," *IEEE Trans. Microwave Theory Tech.*, vol. 42, pp. 2468–2471, Dec. 1994.

[19] A. E. Atia, "Multiple coupled resonator filters synthesis by optimization," in *IEEE MTT-S Int. Microwave Symp. Dig.*, Boston, MA, June 2000, pp. 20–27.

[20] P. Martin and J. Ness, "Coupling bandwidth and reflected group delay characterization of microwave bandpass filters," *Appl. Microw. Wireless*, vol. 11, no. 5, May 1999.

J. Brian Thomas (M'96) received the B.S. degree in physics from Stephen F. Austin State University, Nacogdoches, TX, in 1989, and the M.E.E. degree (with a specialty in applied electromagnetics) from the University of Houston, Houston, TX, in 1992.

From 1992 to 1995, he was an RF Engineer with Microwave Networks Inc., Houston, TX. From 1995 to 2001, he designed filter and duplexer-based products for L3 Communications, Narda West, Sacramento, CA, and for Remec Wacom, Waco, TX. He is currently a Lecturer in the Engineering Department, Baylor University, Waco, TX. He is also an RF consultant. His interests include RF and microwave filters, antennas, and radio astronomy.